Indexed in
*Scopus Compendex and Geobase Elsevier,
Geo-Ref Information Services-USA, List B of Scientific
Journals, Poland, Directory of Research Journals*

International Journal of Earth Sciences and Engineering

www.cafetinnova.org

ISSN 0974-5904, Volume 08, No. 02

April 2015, P.P.550-556

Mapping of Hydrothermal Altered Mineral Zones by Multispectral and Hyper-spectral Data Analysis -A Case Study of Bauchi, Nigeria

SANI IDRIS GARBA AND APARNA S BHASKAR

Department of Civil Engineering, Faculty of Engineering and Technology, SRM University, Kattankulathur-603203, Tamil Nadu, India

Email: *idrisgarbasani@gmail.com*

Abstract: Structural features like faults, shear zones, plugs, dykes and deformities. Present study aims to evaluate and map the altered mineral deposits by analysis of multispectral (Enhanced Thematic Mapper (ETM+)) and hyperspectral (Hyperion) datasets. Various thematic maps were prepared from the ETM+ and ASTER Digital Elevation Model (ASTERDEM), which were used as the input for the finding the final alteration zone mapping. Principal Component Analysis (PCA) and band ratio were also applied to the ETM+ for the detection of altered mineral deposits. A Hyperion image was first compensated for atmospheric effects after the removal of the bad bands from the dataset. Minimum Noise Fraction (MNF) transformation was applied to reduce the data noise and spectral dimensionality. Pixel Purity Index (PPI) and n-Dimensional visualization were used for extracting the pure pixels. These pure pixels are then compared using a mineral spectral library distributed from United States Geological Survey (USGS) as a reference and are used in Spectral Angle Mapping (SAM) to classify the image for identifying the occurrences of same minerals. The results revealed the potential use of Hyperion data over multispectral data in precise altered mineral identification and mapping.

Keywords: *Alteration zones, Principal Component Analysis, Band ratio, Minimum Noise Fraction, Pixel Purity Index, Spectral Angle Mapping.*

1. Introduction

The social and economic development of a nation depends on its capacity to utilize its natural resources. The main demand in the field of mineral exploration is to use new technology to discover new/additional mineral deposits in cost effective manner. The art of remote sensing aids faster identification of mineralized zones and metallogenic belts either directly or indirectly. Alteration zones are created around a number of the structural features like faults, shear zones, plugs, dykes and unconformities, and are defined as either alteration haloes, where the pre-existing rock property values are enhanced or depleted, or as replacement zones.

Alteration zone constitute one of the most important guides for mineral exploration. The major minerals in the alteration zone include carbonates, iron oxide, hydroxyl bearing minerals and tectosilicates. Remote sensing data is of invaluable use in mapping hydrothermally altered rocks because many of the alteration minerals produced have distinctive absorption features caused by the presence of OH, and other hydroxyl bonds: Mg-OH and Al-OH, particularly in the shortwave infrared part of the spectrum (2000–2400 nm) (Hunt 1977). Hence, the present study aims to evaluate and map the altered mineral deposits by analysis of multispectral and hyperspectral data.

2. Study area and Geological setting

The study area (Fig 1) is in the northeast Nigeria, located on the northern edge of the Jos Plateau, with latitudes 9°3' and 12°3' N and longitudes 8°50' and 11° E. The state is bordered by seven states, Kano and Jigawa to the North, Taraba and Plateau to the South, Gombe and Yobe to the East and Kaduna to the West. The Study area is a part of the crystalline rock area in central northern Nigeria. The hill ranges are developed on basement complex rocks in an area which is also characterized by extensive plateau surfaces and volcanic extrusions. The base of the hill ranges is generally at the 600 m level, while peaks rise to 700 m on the hills, and 729 m on the Bunsil hills. A central high plain (of the Hausa land) area belonging to the Kerri Kerri and Gombe sandstone and shale of Tertiary Age.

3. Material and methods

The materials used for this study include the topographical map of Nigeria, geological map, ASTER Digital Elevation Model, Landsat Enhance Thematic Mapper (ETM+) and Hyperion dataset. The Table 1shows the information of the data used. Radiometrically corrected Hyperion data onboard EO-1 satellite Level 1R data is used for the current study.

3.1 Methodology

The whole image processing operation was done in ENVI 4.2 software. Methodology adopted for the present study is depicted in fig 2. Various analyses were carried out for the identification of the structural features and to examine the terrain. The Digital Elevation model obtained from ASTERDEM was used to extract the slope aspect, shaded relief and drainages in the area. ETM+ and Hyperion data were used for analysis for the identification of altered zones. ETM+ image data covering the area to which the Hyperion dataset is available was used for various image processing technique such as PCA, a band ratio for the identification of hydrothermal zones.

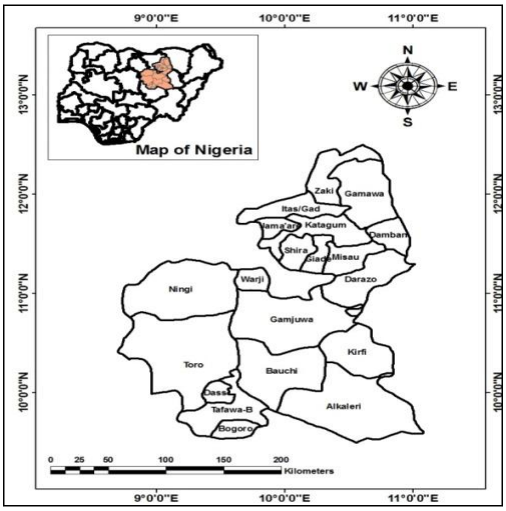

Fig 1: *Location of the study area*

Table1: *Materials and data used*

Data Used	Description
Topographical map of Nigeria	Scale 1:100,000
Geological map of Nigeria	Scale 1:50,000
ASTER Digital Elevation Model	30m spatial resolution
Enhance Thematic Mapper (ETM+)	30 m spatial resolution (band 1-5 and 7), 60 m (band 6) and 15 m (band 8).
Hyperion USGS format L1R Dataset.	242 spectral bands, 10 nm spectral resolution and 30 m spatial resolution

4. Observations and Results

The Digital Elevation Model (Fig. 3) shows the elevation variation in the area. The drainage map shows the different patterns usually control by lithological and structural nature of the area. The drainage density derived from drainage map is shown in fig. 5 which further enhances the lithology and surface structures of the area.

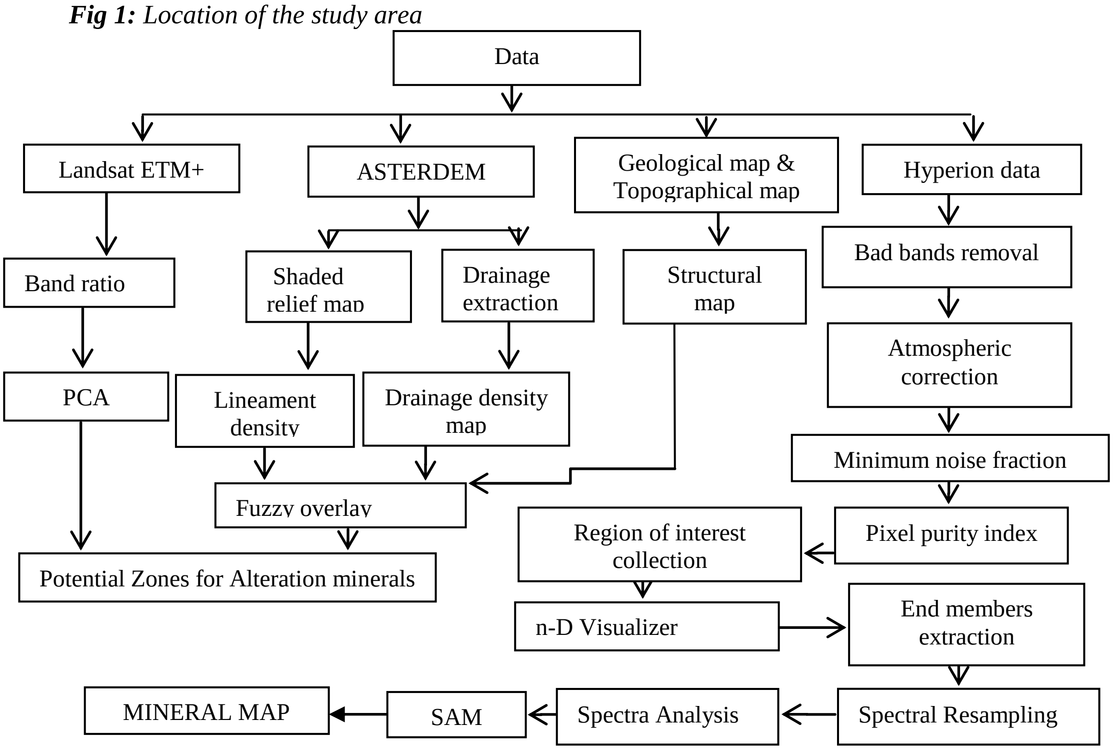

Fig 2. *Methodology flow chart*

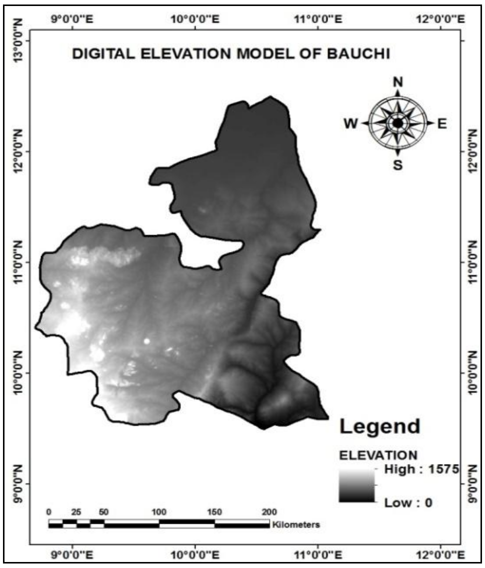

Fig 3. *ASTERDEM*

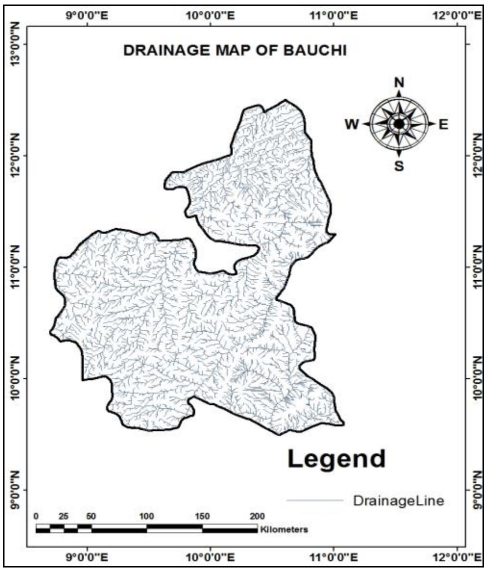

Fig 4. *Drainage map*

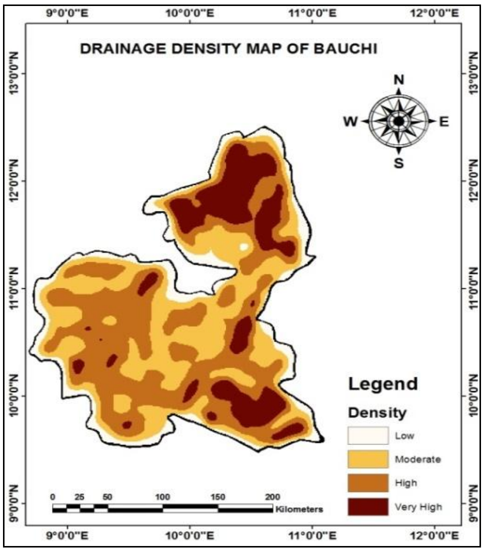

Fig 5: *Drainage Density map*

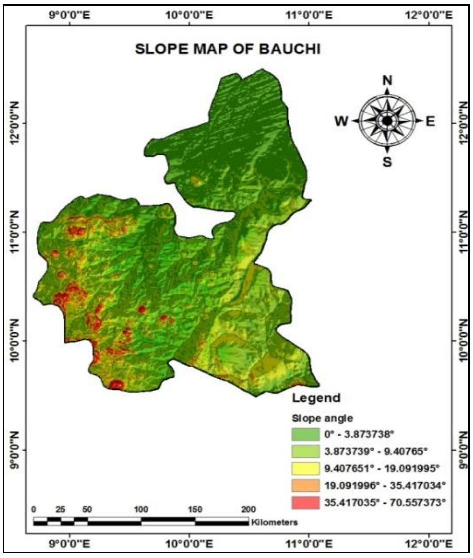

Fig 6. *Slope map*

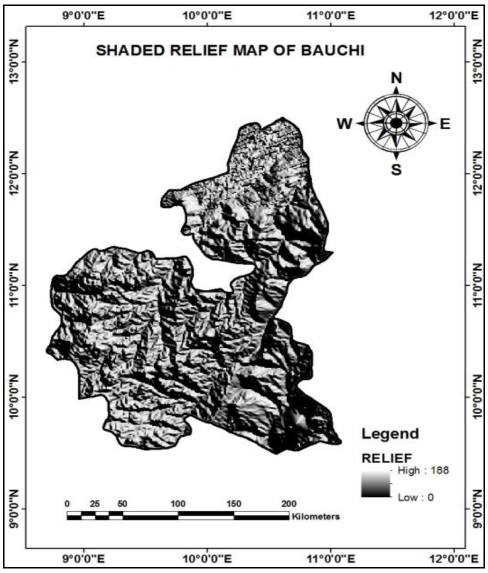

Fig 7.*Superimposed Shaded relief maps*

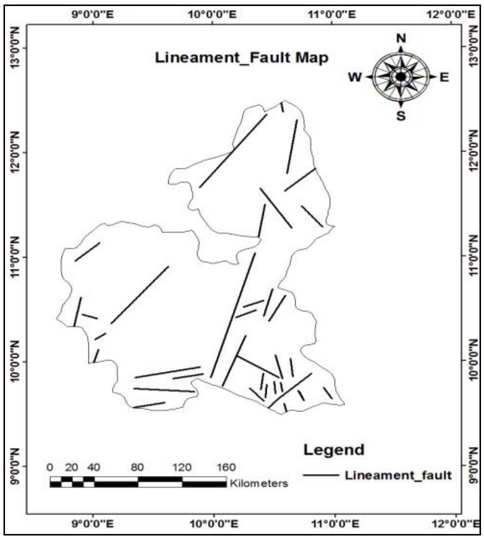

Fig 8. *Lineament-fault map*

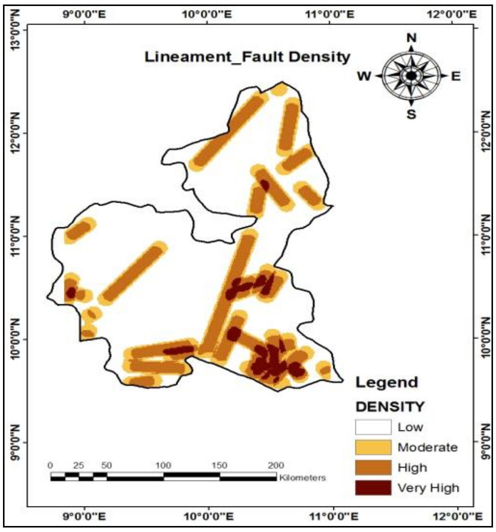

Fig9. *Lineament-fault Density map*

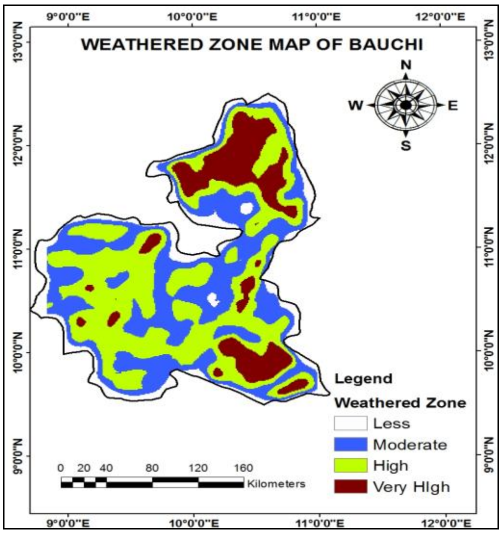

Fig10. *Weathered zone map*

Lineaments (Fig 8) were visually interpreted from Landsat ETM+ images using different image processing technique. Various filtering technique and enhancement has been used for extraction of the lineament. Shaded relief maps at different azimuth (Fig 7) were created from ASTERDEM data of the region and superimposed to enhance nature of the relief which enabled lineament identification. Finally the weathered zones were been identified by overlaying the lineament density and drainage density (Fig 10).

4.1 Band Ratio and Color Composite

The application of band ratio and creation of false colour composite is based on known spectral properties of rocks and alteration minerals in relation to the selected spectral bands. The ratio of the region of interest imageries (fig 12 & 13) were obtained using the following band ratio: Chica – Olma ratio and Kauffman ratio. With the Chica – Olma ratio technique, the band ratios 5/7:5/4:3/1 were obtained and assigned the red, green and blue channels respectively to produce a false colour composite. Similarly band ratios 7/4:4/3:5/7 was obtained for Kauffmann ratio technique, (Bodruddoza Mia and Yasuhiro Fujimitsu 2012).

4.2 Principal Component Analysis

To suppress and separate the erroneous effects of vegetation and unveiling the lithology of the tropical terrain the principal components analysis (PCA) was implemented on specific spectral indices of ETM+ data. Vegetation index (band ratio of 4/3), clay minerals index (band ratio of 5/7), ferric iron oxide index (band ratio of 3/1), and ferrous iron oxide index (band ratio of 5/4) were used to generate PCA image components. The image eigen vectors and eigen values were obtained from PCA using covariance matrix on indices.

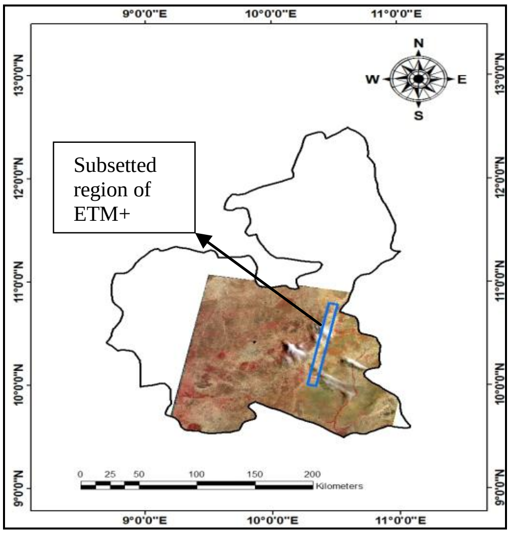

Fig 11: *Subset region of ETM+*

The ETM+ image scene covering the area in which the Hyperion is available (Fig 11) was used for further analysis. The region of interest subsetted from the ETM+ was used for PCA and band ratio to detect the Potential alteration zones (Fig 14).

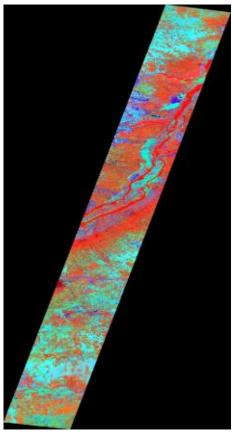

Fig 12.*Chica-Olma Ratio Image (3/1, 5/4, 5/7), Displaying Feric as Red, Ferrous (Fe2+) Iron as Blue and Ferric (Fe3+) Clay as Green.*

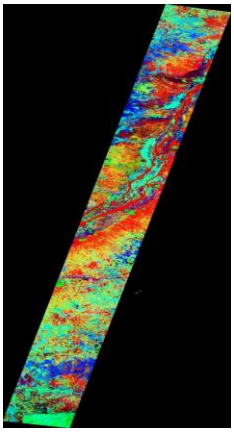

***Fig 13**. Kauffmann Ratio Image (7/4:4/3:5/7), Displaying Iron Minerals as Red, Hydroxyl Minerals as Green*

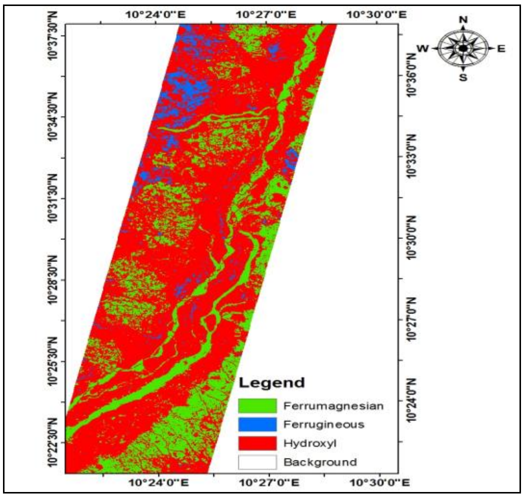

***Fig 14:** Potential alteration zone*

4.3 Bad bands removal

The Hyperion VNIR sensor has 70 bands, and the SWIR has 172 bands providing 242 potential bands. A number of the bands were intentionally not illuminated and others (mainly in the overlap region between the two spectrometers) correspond to areas of low sensitivity of the spectrometer materials (EO1 User guide 2003). The totals of 196 bands were used for the study after removal of unusual bands.

4.4 Atmospheric correction

The Quick Atmospheric Correction model (QUAC) is used in this study to remove this effect and convert the radiance data to reflectance data (Fig15). This algorithm performs automated correction of data in solar reflected region (0.4-2.5um). It creates an image of retrieve surface reflectance, scale into two byte signed integer using reflectance scale factor of 10,000.

4.5 Minimum noise fraction Transformation (MNF)

MNF transformation determines the inherent dimensionality of image data, to segregate noise in the data, and to reduce the computational requirements for subsequent processing. This is a two-step process. First transformations compute the covariance matrix to decorrelate and rescale the noise in the data and its breaks the band to band correlation. Then a second transformation computes the Eigen values, where bands having Eigen values much greater than one contains coherent image and having Eigen values near one contain noise. Using the coherent portion, noise is removed from data (Fig 16). These coherent images will be taken only for further data analysis.

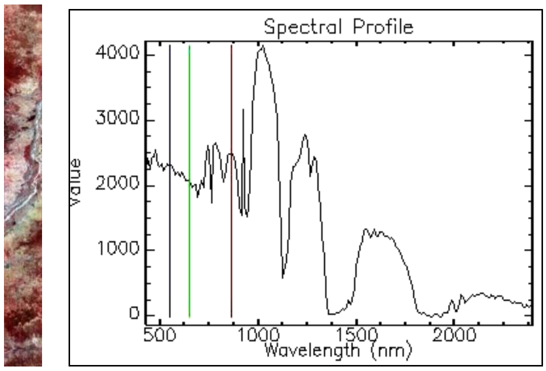

(a) Before atmospheric correction showing vegetation spectral plot

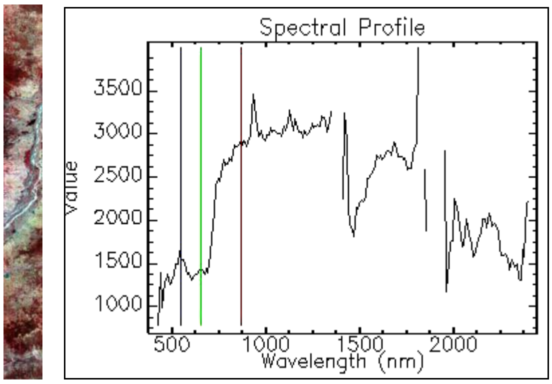

(b) After atmospheric correction showing vegetation spectral plot

***Fig 15.** Showing scene 1 (a) before QUAC atmospheric correction model, (b) after correction*

4.6 Pixel Purity Index (PPI)

The Pixel Purity Index (PPI) is a means of finding the most "spectrally pure," or extreme, pixels in multispectral and hyperspectral images (Boardman et al., 1995). Brighter pixels in the PPI image represent more spectrally extreme pixel and indicate pixels that are more spectrally pure. Darker pixels are less spectrally pure. The PPI is typically run on an MNF transform result; excluding the noise bands. The results of the PPI (Fig.17) are used as input into n-D Visualizer.

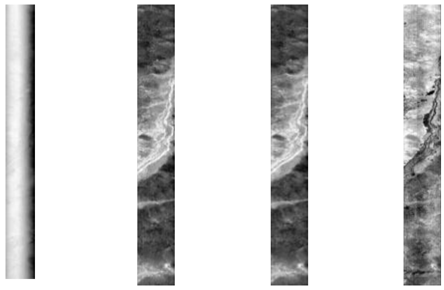

(4268nm-4368nm) (4369nm-4470nm) (4471nm-4572nm) (4573nm-4675nm)

Fig 16. *MNF bands with high Eigen value*

Fig 17. *Pixel Purity Index range*

4.7 The n-Dimensional Visualizer, Spectral Analyst and Spectral Angle Mapping

N-Dimensional Visualizer is used to refine the selection of more spectrally pure endmember class. The selected classes were exported to Region of Interest (ROI) and used as input for further spectral processing. Spectral Analyst uses one or more than one algorithms such as Spectral Angle Mapper, Spectral Feature Fitting and Binary Encoding to measure the similarity between the unknown endmember image spectra and object spectra of the resampled spectral library. Spectral Angle Mapper (SAM) determines the similarity of an unknown spectrum to a reference spectrum by applying the below concept.

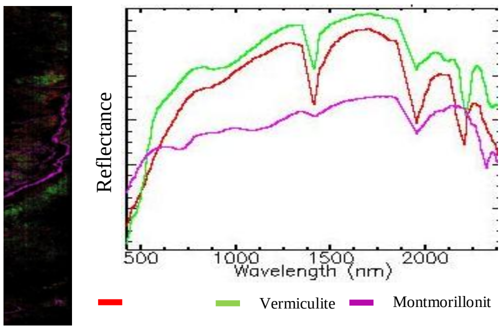

SAM classified image End member Mineral spectral plot

Fig 18. *Mineral Index Map*

5. Results and Discussions

After analyzing the results of PCA transformation for specific spectral indices of ETM+ data, considering magnitude and sign of the eigenvector loadings and percentage of eigenvalues for two scenes, it was realized that the first principal component (PC1) of accounts 87.25 percent of total eigenvalue , which is higher value among the PCA images in the scene. A PCA image with higher eigenvalue contains most of the spectral information in the scene. All of the eigenvector loadings for the PC1 are positive, thus the differentiation between materials (vegetation and alteration minerals) using the specific spectral indices in the PC1 image will be extremely difficult. PC2 show high positive value for ferric iron index (3/1) because of the less vegetation cover in the scene.

Eigen vector loadings for the vegetation index (-0.077) and positive eigenvector loadings for the clay mineral index (0.670). The band ratio indices were applied to PCA images to obtain the potential altered zone (Fig 14). Finally mineral map was created using spectral angle mapper classifier algorithm in which three mineral types were identified in the area (Fig. 18). The minerals are vermiculite, montmorillonite and koasmec (koalonite+smectite).

6. Conclusions

The results presented in this study demonstrate the potential of hyperspectral image data over multispectral data in precise mapping of altered mineral zones. Structurally controlled mineralization like clay mineral has been detected using hyperspectral data in this study. The same methodology can be further adopted for mapping of other altered minerals. Having the same spatial resolution in compare to other multispectral data, the Hyperion data provided the advantage of high-quality reflectance spectra of the surgical features. The limits of the Hyperion imagery for mineral mapping are the apparent strips in several bands even those important absorption bands and the low signal-to-noise ratio of imagery.

It can be concluded that the Hyperion data has the capability of identifying the precise altered mineral because of its high spectral information when compared to the ETM+ which is only to map the alteration zones.

References

[1] Ali E.A., El Khidir S.O., Babikir I. A.A. and Abdelrahman E.M. (2012) "*Landsat ETM+7 Digital Image Processing Techniques for Lithological and Structural Lineament Enhancement: Case Study Around Abidiya Area, Sudan*" The Open Remote Sensing Journal, pp 5, 83-89, 2012.

[2] Amina Kassou, Ali Essahlaoui and Mohamed Aissa (2012) "*Extraction of Structural Lineaments from Satellite Images Landsat 7*

ETM+ of Tighza Mining District (Central Morocco)" Research Journal of Earth Sciences 4 (2): pp 44-48, 2012.

[3] Eirini S. Papadaki, Stelios P. Mertikas, and Apostolos Sarris (2011) "*Identification of lineaments with possible structural origin using Aster images and Dem derived products in western Crete, Greece*" EARSeL eProceedings 10, 1/2011, pp 9,2011.

[4] El-Nahry A.H. and Altinbas U. (2006) "*Processing and Analyzing Advanced Hyperspectral Imagery Data for Identifying Clay Minerals. A Case Study*" Journal of Applied Science Research 2 (4): pp. 232-238,2006.

[5] Ezekwesili Godwin ENE, Celestine Obialo OKOGBUE, Chidozie Izuchukwu Princeton DIM (2012) "*Structural styles and economic potentials of some barite deposits in the Southern Benue Trough, Nigeria"* Romanian Journal of Earth Sciences, vol. 86 (2012), issue 1, p. 27-40, 2012.

[6] Fatoye F. B. and Gideon Y. B. (2013) "*Geology and mineral resources of the Lower Benue Trough, Nigeria"* Advances in Applied Science Research, 4(6): pp21-28, 2013.

[7] Fred A. Kruse, Sandra L. Perry and Alejandro Caballero (2006) "*District-level mineral survey using airborne hyperspectral data, Los Menucos, Argentina*" Annals of Geophysics, vol. 49, No.1pp 83-92, 2006.

[8] Gongwen Wang, Yuqi liang "*Hydrothermal alteration mapping based on MPH and fractal technologies using ASTER and ETM+ data in Lushi region, Henan Province, China"* 2nd Conference on Environmental Science and Information Application Technology pp762-765.

[9] Ikoro D. O., Agumanu A.E. and Okereke C. N. (2012) "*Tectonic and paleoenvironmental significance of clay mineral suites in the southern Benue trough"* International Journal of Emerging trends in Engineering and Development Issue 2, Vol.2 pp 1-5,2012.

[10] Jibran Khan (2013) "*Hyperspectral Image analysis for Dolomite Identification in Tarbela Dam Region of Pakistan".* International Journal of Innovative Technology and Exploring Engineering (IJITEE) Volume-2, Issue-3, pp 30-34, 2013.

[11] Kudamnya E. A, andongma W. T & Osumeje J. (2014) "*hydrothermal mapping of Maru schist belt, north-western Nigeria using remote sensing technique".* International Journal of Civil Vol. 3, pp 59-66, 2014.

[12] Magendran T. and Sanjeevi S. (2013) "*A Study on the Potential of Satellite Image-derived Hyperspectral Signatures to Assess the Grades of Iron ore Deposits*" Journal Geological Society of India Vol.82, September 2013, pp.227-235.

[13] Pour1and A B and Hashim M (2014) "*Alteration mineral mapping using ETM+ and Hyperion remote sensing data at Bau Gold Field, Sarawak, Malaysia*". 8th International Symposium of the Digital Earth (ISDE8). IOP Conf. Series: Earth and Environmental Science 18 (2014) pp 1-5

[14] Rajat Satpathy, Vivek Kumar Singh, Reshma Parveen, Ayyem Thillai Jeyaseelan (2010)" *Spectral Analysis of Hyperion Data for Mapping the Spatial Variation of AL+OH Minerals in a Part of Latehar & Gumla District, Jharkhand"* Journal of Geographic Information System, pp 2, 210-214.

[15] Ronen Gersman, Eyal Ben-Dor, Michael Beyth, Dov Avigad, Michael Abraha & Alem Kibreab (2008) "*Mapping of hydrothermally altered rocks by the EO-1 Hyperion sensor, Northern Danakil Depression, Eritrea*" International Journal of Remote Sensing Vol. 29, No. 13, 10 July 2008, 3911–3936.

[16] Salaj .S.S, Richa Upadhyay, Srivastav S. K., Prabhakaran (2012) "*Mineral Abundance Mapping Using Hyperion Dataset in Part of Udaipur District Rajasthan, India".*14th Annual international conference and exhibition on Geospatial information technology and application.

[17] Sharma Kiran Kumari, Chakravarty Debashish, Das Pulakesh and Bandhopadhyay Jatisankar (2014) "*Hyperion Image Analysis for Iron Ore Mapping in Gua Iron Ore Region, Jharkhand, India*" International Research Journal of Earth Sciences, Vol. 2(9), pp 1-6, 2014.